Impaired Store-Operated Calcium Entry and STIM1 Loss Lead to Reduced Insulin Secretion and Increased Endoplasmic Reticulum Stress in the Diabetic β-Cell

Tatsuyoshi Kono,[1,2] Xin Tong,[3] Solaema Taleb,[1] Robert N. Bone,[1] Hitoshi Iida,[1] Chih-Chun Lee,[1] Paul Sohn,[4] Patrick Gilon,[5] Michael W. Roe,[6] and Carmella Evans-Molina[1,2,4,7,8]

Diabetes 2018;67:2293–2304 | https://doi.org/10.2337/db17-1351

Store-operated Ca^{2+} entry (SOCE) is a dynamic process that leads to refilling of endoplasmic reticulum (ER) Ca^{2+} stores through reversible gating of plasma membrane Ca^{2+} channels by the ER Ca^{2+} sensor Stromal Interaction Molecule 1 (STIM1). Pathogenic reductions in β-cell ER Ca^{2+} have been observed in diabetes. However, a role for impaired SOCE in this phenotype has not been tested. We measured the expression of SOCE molecular components in human and rodent models of diabetes and found a specific reduction in STIM1 mRNA and protein levels in human islets from donors with type 2 diabetes (T2D), islets from hyperglycemic streptozotocin-treated mice, and INS-1 cells (rat insulinoma cells) treated with proinflammatory cytokines and palmitate. Pharmacologic SOCE inhibitors led to impaired islet Ca^{2+} oscillations and insulin secretion, and these effects were phenocopied by β-cell STIM1 deletion. STIM1 deletion also led to reduced ER Ca^{2+} storage and increased ER stress, whereas STIM1 gain of function rescued β-cell survival under proinflammatory conditions and improved insulin secretion in human islets from donors with T2D. Taken together, these data suggest that the loss of STIM1 and impaired SOCE contribute to ER Ca^{2+} dyshomeostasis under diabetic conditions, whereas efforts to restore SOCE-mediated Ca^{2+} transients may have the potential to improve β-cell health and function.

Reductions in β-cell endoplasmic reticulum (ER) calcium (Ca^{2+}) levels contribute to the pathophysiology of both type 1 diabetes and type 2 diabetes (T2D) and lead to decreased insulin secretion, activation of intracellular stress pathways, and β-cell death. Steady-state ER Ca^{2+} levels are maintained by the balance of Ca^{2+} transport into the ER lumen by the sarco-ER Ca^{2+} ATPase (SERCA) pumps and Ca^{2+} release via the inositol triphosphate receptors and ryanodine receptors (RyRs) (1–4). ER Ca^{2+} depletion also triggers a tightly regulated rescue mechanism that serves to replenish ER Ca^{2+} stores through a family of channels referred to as store-operated or Ca^{2+} release–activated channels (5–7). This process, known as store-operated Ca^{2+} entry (SOCE), is initiated by the dissociation of Ca^{2+} from the ER Ca^{2+} sensor, Stromal Interaction Molecule 1 (STIM1), followed by STIM1 oligomerization and translocation to the ER/plasmalemmal junctional regions (8). Here, STIM1 complexes with selective Orai Ca^{2+} channels (9) and nonspecific transient receptor potential canonical channel 1 (TRPC1), leading to the activation of Ca^{2+} influx from the extracellular space, with subsequent transfer of Ca^{2+} into the ER lumen (10,11). Although pathologic reductions in SERCA-mediated ER Ca^{2+} uptake and dysregulated RyR-mediated ER Ca^{2+} leakage have been described in the diabetic β-cell (4,12,13), a role for impaired β-cell SOCE in this phenotype remains untested.

[1]Department of Medicine, Indiana University School of Medicine, Indianapolis, IN
[2]Richard L. Roudebush VA Medical Center, Indianapolis, IN
[3]Department of Molecular Physiology and Biophysics, Vanderbilt University, Nashville, TN
[4]Department of Cellular and Integrative Physiology, Indiana University School of Medicine, Indianapolis, IN
[5]Pôle d'endocrinologie, diabète et nutrition, Institut de recherche expérimentale et clinique, Université catholique de Louvain, Brussels, Belgium
[6]Department of Medicine, SUNY Upstate Medical University, Syracuse, NY
[7]Department of Biochemistry and Molecular Biology, Indiana University School of Medicine, Indianapolis, IN
[8]Herman B Wells Center for Pediatric Research, Indiana University School of Medicine, Indianapolis, IN

Corresponding author: Carmella Evans-Molina, cevansmo@iu.edu, or Tatsuyoshi Kono, konot@iu.edu.

Received 9 November 2017 and accepted 8 August 2018.

This article contains Supplementary Data online at http://diabetes.diabetesjournals.org/lookup/suppl/doi:10.2337/db17-1351/-/DC1.

In other cell types, SOCE Ca^{2+} transients have been implicated in a number of signaling pathways, including those that regulate proliferation, growth, inflammation, apoptosis, and lipogenesis. In addition, defective SOCE has been associated with several clinical syndromes, including immunodeficiency, myopathy, Alzheimer disease, and vascular disease (14–18). Recently, pharmacologic inhibitors of SOCE or dominant-negative forms of either Orai1 or TRPC1 were shown to decrease insulin secretion in rat islets and clonal β-cell lines (11), while STIM1 was also shown to interact with the sulfonylurea receptor 1 subunit of the K_{ATP} channel and regulate β-cell K_{ATP} activity (19).

Given these recent implications of SOCE in the regulation of insulin secretion, we hypothesized that dysfunctional β-cell SOCE may likewise contribute to diabetes pathogenesis. To this end, we profiled SOCE and the expression of SOCE molecular components in multiple diabetic models, including islets from streptozotocin (STZ)-treated mice, human and mouse islets and rat insulinoma (INS-1) cells treated with proinflammatory cytokines, INS-1 cells treated with palmitate, and human islets isolated from donors with T2D. Our data revealed a preferential loss of STIM1 expression but preserved expression of Orai1 across these models. Moreover, β-cell STIM1 loss as well as STIM1 knockdown led to impaired glucose-stimulated Ca^{2+} oscillations and insulin secretion, and increased β-cell susceptibility to ER stress, whereas STIM1 gain of function rescued these defects. Taken together, these data define a novel role for altered SOCE in diabetes and suggest that efforts to restore STIM1 expression and/or SOCE-mediated Ca^{2+} transients have the potential to improve β-cell function and health.

RESEARCH DESIGN AND METHODS

Reagents

Mouse and human interleukin-1β (IL-1β), interferon-γ (IFN-γ), and tumor necrosis factor-α (TNF-α) were obtained from Invitrogen (Carlsbad, CA); and 2-aminoethoxydiphenyl borate (2-APB), 1-(5-chloronaphthalene-1-sulphonyl)-^{1}H-hexahydro-1,4-diazepine (ML-9), and tunicamycin (TM) were obtained from Tocris Bioscience (Bristol, U.K.). Adenoviruses expressing STIM1 and Cre recombinase were from ViraQuest Inc. (North Liberty, IA) (19). Small interfering RNAs (siRNAs) were obtained from GE Healthcare (Lafayette, CO); and all other chemicals were from Sigma-Aldrich (St. Louis, MO). Supplementary Tables 1 and 2 contain a complete list of PCR primers and antibodies.

Animals and Human Islets

Male C57BL/6J mice were obtained from The Jackson Laboratory (Bar Harbor, ME). At 8 weeks of age, C57BL/6J were injected intraperitoneally with 50 mg/kg STZ or normal saline daily for 5 days. Mice with *loxP* sites flanking exon 2 of the *Stim1* gene were obtained from The Jackson Laboratory and backcrossed onto a C57BL/6J background for at least 10 generations. Mice were maintained under protocols approved by the Indiana University Institutional Animal Care and Use Committee. Cages were kept in a standard light/dark cycle with ad libitum access to food and water.

Cadaveric human islets from donors without diabetes and donors with T2D were obtained from the Integrated Islet Distribution Program. The data presented include the analysis of islets from 8 donors without diabetes (5 female; 3 male) and 11 donors with T2D (7 female; 4 male). The average age (±SEM) of the donors without diabetes was 45.9 ± 10.3 years; the mean BMI was 25.6 ± 4.7 kg/m^2. The average age of donors with T2D was 50.9 ± 8.9 years; the average BMI was 33.2 ± 7.1 kg/m^2.

Cell Culture and Islet Treatments

Rat INS-1 832/13 cells and human and mouse pancreatic islets were cultured as previously described (20,21). CRISPR/Cas9 genomic editing was used to create a STIM1 knockout (KO) INS-1 832/13 cell line in the Genome Engineering and iPSC Center at Washington University (St. Louis, MO). To mimic proinflammatory and diabetic conditions, INS-1 cells were treated with 5 ng/mL IL-1β, and mouse and human islets were treated with 5 ng/mL IL-1β, 100 ng/mL IFN-γ, and 10 ng/mL TNF-α for 24 h as previously published (12). To induce ER stress, INS-1 cells were treated with 10 μmol/L TM for 3–24 h. For viral transduction studies, 50–100 islets were handpicked within 1 h of isolation or receipt, incubated with adenovirus for 16 h, followed by an additional 48–72 h of incubation in fresh medium without adenovirus. To obtain STIM1 KO islets, isolated islets from STIM$^{flox/flox}$ mice were transduced with an adenovirus encoding Cre recombinase under control of the cytomegalovirus promoter. Glucose-stimulated insulin secretion (GSIS), immunoblot, and immunofluorescence in cultured wild-type (WT) INS-1 cells, STIM1 KO cells, and isolated mouse and human islets were performed as previously described (4,12). Islet GSIS was also measured using the Biorep Perifusion System (Biorep, Miami Lakes, FL) (22). Twenty-four hours after isolation, 50 handpicked islets were loaded into each perifusion chamber; islets were perifused with Krebs buffer containing 2.8 mmol/L glucose for 20 min, followed by 16.7 mmol/L glucose for 40 min at a rate of 120 μL/min. Secreted insulin was measured using an ELISA (Mercodia, Uppsala, Sweden); results were normalized to DNA content. Quantitative real-time (qRT)-PCR was performed using previously published primer sequences (23) or primers outlined in Supplementary Table 1. To generate transmission electron micrographic images, INS-1 cells were fixed in 2% glutaraldehyde and 4% paraformaldehyde in 0.1 mol/L sodium cacodylate buffer and transferred to the Advanced Electron Microscopy Facility at the University of Chicago (Chicago, IL).

Live Cell Imaging

Cytosolic Ca^{2+} dynamics in INS-1 cells were measured using the FLIPR Calcium 6 Assay Kit and a FlexStation

3 Plate Reader (Molecular Devices, Sunnyvale, CA). To measure SOCE, INS-1 832/13 β-cells were loaded with Calcium 6 in growth medium containing 11 mmol/L glucose for 2 h. Immediately prior to Ca^{2+} imaging, cells were incubated in Ca^{2+}-free Hanks' balanced salt solution (HBSS) with the following composition: 138 mmol/L NaCl, 5.3 mmol/L KCl, 0.34 mmol/L Na_2HPO_4, 0.44 mmol/L KH_2PO_4, 4.17 mmol/L $NaHCO_3$, and 5.5 mmol/L glucose for 4 min. Ca^{2+} imaging experiments were performed according to the strategy shown in Fig. 1*A*. Baseline fluorescence (F0) was measured for a minimum of 10 s under Ca^{2+}-free conditions and in the presence of 0.5 mmol/L EGTA (Ca^{2+} chelator), 10 μmol/L verapamil (L-type voltage-dependent Ca^{2+} channel blocker), and 200 μmol/L diazoxide (K_{ATP} channel opener applied to prevent voltage-dependent Ca^{2+} channel activation). Next, thapsigargin (TG; a SERCA inhibitor) was used to empty ER Ca^{2+} stores, followed by supplementation with 2 mmol/L Ca^{2+} in the media. SOCE was detected as an elevation of Calcium 6 intensity (vertical red arrow; ΔF)

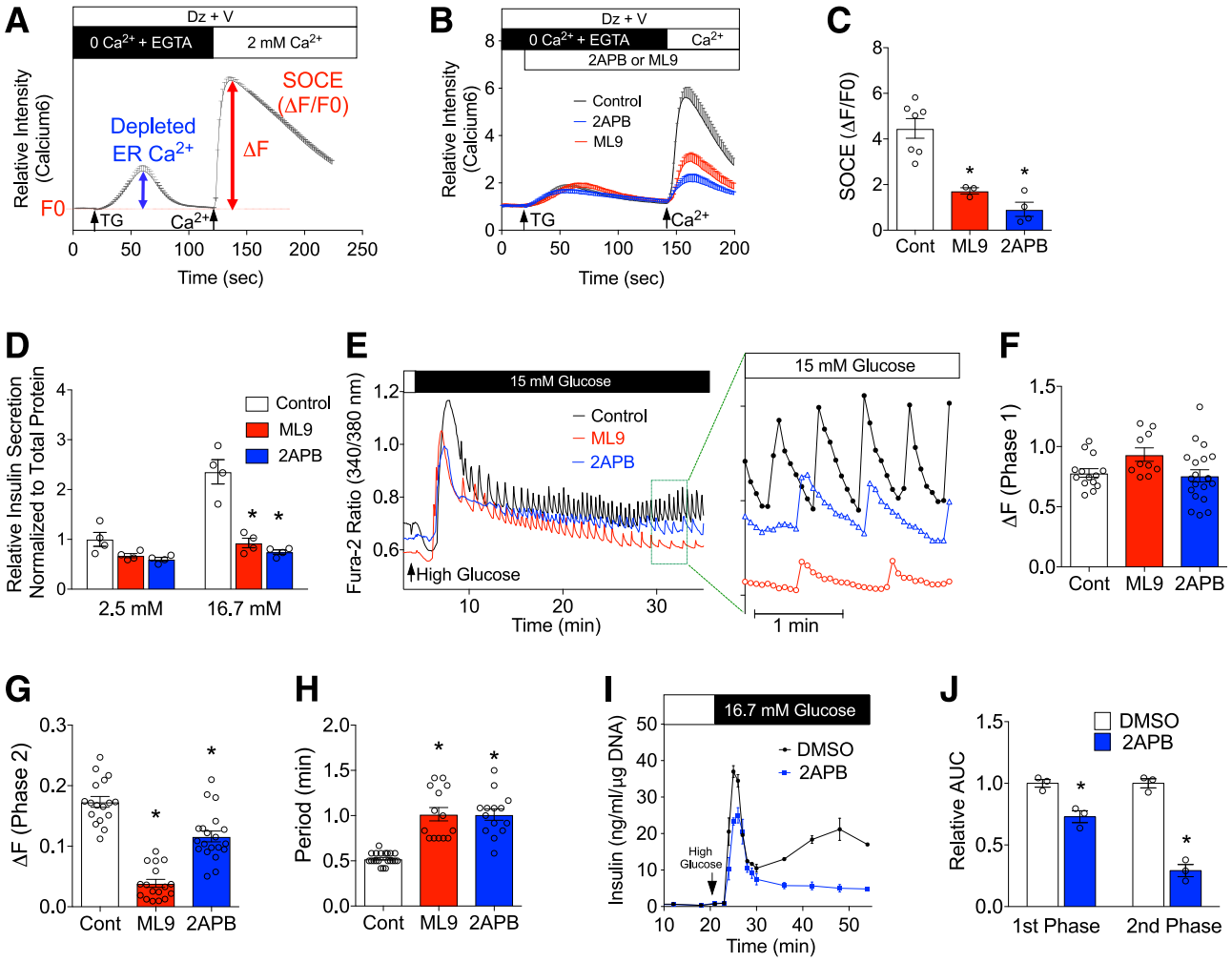

Figure 1—Pharmacologic inhibition of SOCE led to impaired insulin secretion and glucose-induced Ca^{2+} oscillations. *A*: INS-1 832/13 β-cells were loaded with Calcium 6, and Ca^{2+} imaging experiments were performed to measure SOCE, according to the strategy shown. *B* and *C*: Ca^{2+} imaging was performed with or without known SOCE inhibitors, 50 μmol/L ML-9 and 200 μmol/L 2-APB, in the presence of 5.5 mmol/L glucose, 200 μmol/L diazoxide, and 10 μmol/L verapamil (Dz + V). ER Ca^{2+} depletion was induced with 3 μmol/L TG, and SOCE was quantified as the cytosolic Ca^{2+} increase after supplementation with 2 mmol/L Ca^{2+}. Results were displayed as the ΔF/F0 after Ca^{2+} supplementation. *D*: GSIS was measured in INS-1 cells pretreated with or without ML-9 and 2-APB and normalized to total protein content. *E–H*: Glucose-stimulated Ca^{2+} imaging was performed using Fura-2 AM in islets isolated from C57BL/6J mice and pretreated with ML-9 or 2-APB. *E*: Representative cytosolic Ca^{2+} recording after stimulation with 15 mmol/L glucose. Quantification of the average phase 1 amplitude (*F*), phase 2 (oscillation) amplitude (*G*), and oscillation period (*H*). *I*: Mean insulin concentration profiles during islet perifusion at basal 2.8 mmol/L glucose concentrations (0–20 min) and in response to 16.7 mmol/L glucose stimulation (20–60 min). DMSO or 200 μmol/L 2-APB was added to the 16.7 mmol/L glucose buffer. Fifty islets were loaded per chamber, and data are reported as ng/mL insulin normalized to islet DNA content ($n = 3$). *J*: Relative area under curve (AUC) values for first phase (20–30 min) and second phase (30–60 min) insulin secretion with DMSO and 2-APB treatment. The numbers of replicates for each experiment are indicated by the open circles. Results are displayed as the means ± SEM; $^*P < 0.05$ compared with control (Cont) conditions.

in response to Ca^{2+} addition, which was normalized to the basal F0 (red dotted line), according to the formula ΔF/F0. Cytosolic Ca^{2+} imaging was performed in isolated islets incubated in HBSS buffer supplemented with 2 mmol/L Ca^{2+} and the ratiometric Ca^{2+} indicator fura-2-acetoxymethylester (Fura-2 AM) (Life Technologies) using a Zeiss Z1 microscope as previously described (4,24).

To directly image ER Ca^{2+} levels, cells were transfected with an adenovirus encoding the ER-targeted D4ER probe expressed under the control of the rat insulin promoter (23). Fluorescence lifetime imaging microscopy (FLIM) was used to monitor steady-state ER Ca^{2+} levels in accordance with previously published protocols (4,25). For Förster resonance energy transfer (FRET) experiments, confocal images were acquired with a Leica TCS SP8 confocal/multiphoton imaging system (Leica Microsystems, Inc., Buffalo Grove, IL). Imaging was performed using a 448-nm single excitation laser line, and fluorescent emission collected with two hybrid detectors set to 460–500 and 515–550 nm emission slit widths. Time series images (*z* stacks) of two to three stage-registered fields were acquired over a period of 20 min. Images were analyzed using Leica LAS X software (version 3.3) to calculate the change in FRET ratio over time.

Statistical Analysis

Differences between groups were examined for significance using either a two-tailed Student *t* test or one-way ANOVA followed by the Tukey-Kramer post-test using GraphPad Prism statistics software (GraphPad Software, Inc., San Diego, CA). Pearson correlations were used to analyze the relationships between STIM1 mRNA levels and donor BMI. Unless indicated, results were displayed as the mean ± SEM; a P value of <0.05 was used to indicate a significant difference between groups.

RESULTS

Pharmacologic Inhibition of SOCE Impaired Glucose-Stimulated Ca^{2+} Oscillations and Insulin Secretion

To image β-cell SOCE, INS-1 cells were loaded with Calcium 6; Ca^{2+} imaging experiments were performed according to the schematic shown in Fig. 1*A* and described in the RESEARCH DESIGN AND METHODS. As shown previously (26,27), pharmacologic SOCE inhibitors ML-9 and 2-APB reduced the ΔF/F0 activated in response to ER Ca^{2+} depletion (Fig. 1*B* and *C*). Moreover, ML-9 and 2-APB reduced GSIS by 61% and 68%, respectively, in INS-1 β-cells (Fig. 1*D*). To test whether SOCE inhibitors similarly impacted glucose-stimulated Ca^{2+} oscillations, islets from WT C57BL/6J mice were treated with either ML-9 or 2-APB and then loaded with Fura-2 AM for the analysis of glucose-stimulated Ca^{2+} responses (Fig. 1*E*). Although pharmacologic inhibition of SOCE had no effect on the phase 1 ΔF response to glucose (Fig. 1*F*), ML-9 and 2-APB reduced the average amplitude of the oscillatory response (ΔF phase 2) and increased the oscillatory period (Fig. 1*G* and *H*). In islet perifusion experiments, the addition of 2-APB to the high-glucose buffer significantly reduced both first- and second-phase insulin secretion (Fig. 1*I* and *J*). Consistent with the effects observed on glucose-stimulated Ca^{2+} oscillations, a more striking effects was observed on second-phase insulin secretion.

β-Cell STIM1 Expression Was Reduced in Mouse and Human Models of Diabetes

Next, islets were isolated from STZ or saline-treated C57BL/6J mice and glucose-stimulated Ca^{2+} imaging performed. Islets from STZ-treated mice had reduced amplitude of the ΔF phase 1 and 2 responses and a decreased oscillatory period (Fig. 2*A*–*E*). To test whether observed changes in calcium signaling may be related to changes in the expression of the molecular components of the β-cell SOCE complex, first, we compared the expression levels of STIM and Orai isoforms in human and mouse islets and INS-1 cells (Supplementary Fig. 1*A*–*C*). In human islets, mouse islets, and INS-1 cells, STIM1 was expressed at higher levels compared with STIM2. Orai2 was the most highly expressed Orai isoform in human islets. In mouse islets, Orai1 and Orai3 levels were nearly equivalent, and these were the most abundantly expressed Orai isoforms. Orai3 was the mostly highly expressed isoform in INS-1 cells. Analysis of islets from STZ-treated mice revealed a specific reduction in STIM1 gene and protein expression (Fig. 2*F*–*H*), whereas no differences in *STIM2*, *Orai1*, *Orai2*, or *Orai3* gene expression were observed between saline and STZ-treated groups (Fig. 2*F*).

Homozygous STIM1 KO mice experience perinatal lethality, and STIM2 KO mice die shortly after birth (28,29). To test whether KO of STIM1 was sufficient to impair glucose-stimulated Ca^{2+} responses, islets from $STIM1^{flox/flox}$ mice were transduced with an adenovirus encoding Cre recombinase. STIM1 protein was effectively reduced in Cre-transduced islets from $STIM^{flox/flox}$ mice (pSTIM1KO) (Fig. 2*I*). Consistent with the results observed in islets isolated from STZ-treated mice, the amplitude of the phase 1 and 2 responses were reduced in pSTIM1KO islets (Fig. 2*J*–*M*). Similar to the results obtained in islets from STZ-treated mice, the oscillatory period was also reduced in pSTIM1KO islets (Fig. 2*E* and *N*). However, this was noted to be in contrast to the increased oscillatory period observed in islets treated with ML-9 or 2-APB (Fig. 1*H*).

Next, we tested whether the expression of SOCE molecular constituents was altered in islets from human cadaveric donors with T2D. This analysis revealed a significant reduction in *STIM1* and *Orai2* gene expression and a trend toward reduced Orai1 mRNA expression in islets from donors with T2D (P = 0.06) (Fig. 3*A*). Immunoblot analysis revealed no change in Orai1 or Orai2 protein levels (data not shown), but STIM1 protein expression was reduced by ∼40% in islets from donors with T2D (Fig. 3*B* and *C*). Next, Pearson correlation tests were used to assess the relationships between donor BMI and *STIM1* mRNA levels. In islets from donors without diabetes, *STIM1* mRNA levels were positively correlated

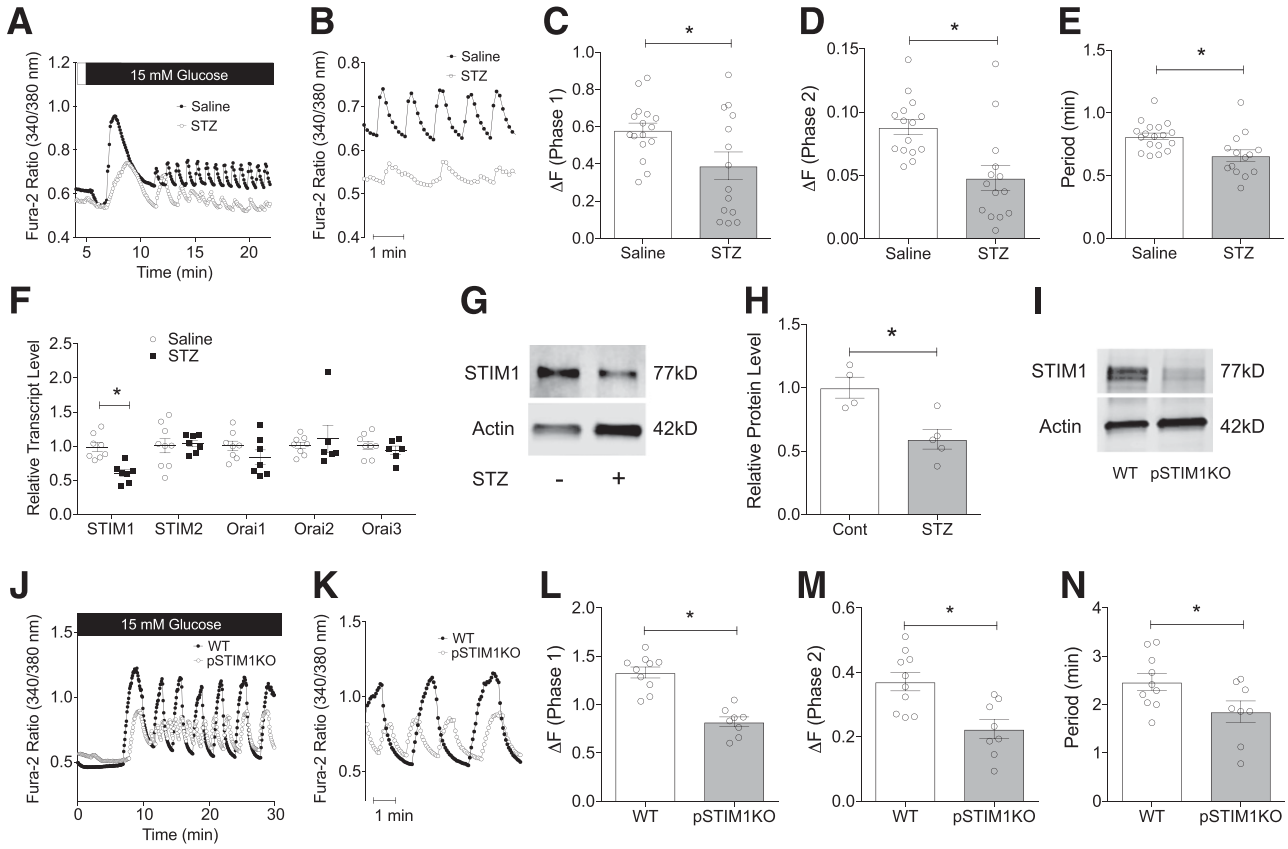

Figure 2—Loss of STIM1 expression led to impaired islet glucose–stimulated Ca^{2+} oscillations. Islets were isolated from saline and STZ-treated C57BL/6J mice and loaded with Fura-2 AM for Ca^{2+} imaging experiments in the presence of 5.5 mmol/L glucose. *A* and *B*: Representative cytosolic Ca^{2+} recording of islets after stimulation with 15 mmol/L glucose. Quantification of the average phase 1 amplitude (*C*), phase 2 (oscillation) amplitude (*D*), and phase 2 period (*E*). *F–H*: Islets were isolated from saline and STZ-treated C57BL/6J mice. *F*: Total islet RNA was subjected to qRT-PCR for the quantification of STIM and Orai isoform mRNA expression levels (normalized to actin mRNA expression). *G* and *H*: Immunoblot was performed using antibodies against STIM1 and actin. Shown is a representative immunoblot and the mean ± SEM of STIM1 protein levels from multiple replicates. *$P < 0.05$ compared with islets from saline-treated mice. *I–N*: Islets isolated from $STIM1^{flox/flox}$ mice were transduced with a Cre-expressing adenovirus (pSTIM1KO) or empty viral control (WT). *I*: Reduced STIM1 protein expression in pSTIM1KO islets was confirmed by immunoblot. *J–N*: pSTIM1KO islets were loaded with Fura-2 AM, and Ca^{2+} imaging was performed. *J* and *K*: Representative cytosolic Ca^{2+} recording after stimulation with 15 mmol/L glucose. Quantification of the average phase 1 amplitude (*L*), phase 2 (oscillation) amplitude (*M*), and oscillation period (*N*); $n = 4–5$ per group. *$P < 0.05$ compared with WT islets. Numbers of replicates for each experiment are indicated by the open circles. Cont, control.

with BMI (R^2 = 0.573; P = 0.048), whereas this correlation was lost in donors with T2D (Fig. 3*D*).

Proinflammatory Cytokine Stress Reduced β-Cell STIM1 mRNA and Protein Expression and Led to Impaired SOCE

To define whether STIM1 expression was similarly impacted under in vitro diabetic stress conditions, human and mouse islets were treated with a mixture of proinflammatory cytokines, consisting of 5 ng/mL IL-1β, 100 ng/mL IFN-γ, and 10 ng/mL TNF-α for 24 h Cytokine treatment led to a significant reduction in STIM1 protein levels in human and mouse islets (Fig. 4*A* and *B*). Because INS-1 cells are known to be more sensitive to proinflammatory cytokines (30), INS-1 cells were treated with increasing doses of IL-1β alone for 24 h. Consistent with the results obtained in human and mouse islets, STIM1 protein and mRNA levels decreased significantly with IL-1β treatment (Fig. 4*C–E*), whereas no reductions in *STIM2*, *Orai1*, *Orai2*, or *Orai3* mRNA expression were observed (Fig. 4*C*). Reduced STIM1 expression correlated with a dose-dependent reduction in SOCE (Fig. 4*F* and *G*). Quantitation of the ΔF in response to TG was reduced in parallel, suggesting impaired ER Ca^{2+} storage in IL-1β–treated INS-1 cells (Fig. 4*H*).

To test these findings in another model of diabetic stress, INS-1 cells were treated with 0.5 mmol/L palmitate combined with 25 mmol/L glucose to mimic glucolipotoxicity (GLT). In GLT-treated INS-1 cells, both STIM1 and STIM2 mRNA levels were reduced (Fig. 4*I*), and STIM1 protein was reduced in parallel (Fig. 4*J*). No significant change in Orai1–3 mRNA levels was observed. SOCE was significantly decreased by GLT treatment as well as palmitate treatment alone (Fig. 4*K* and *L*). Similar to the results observed with IL-1β treatment, the ΔF response to TG was reduced in both palmitate and GLT-treated INS-1 cells (Fig. 4*K* and Supplementary Fig. 2*A* and *B*).

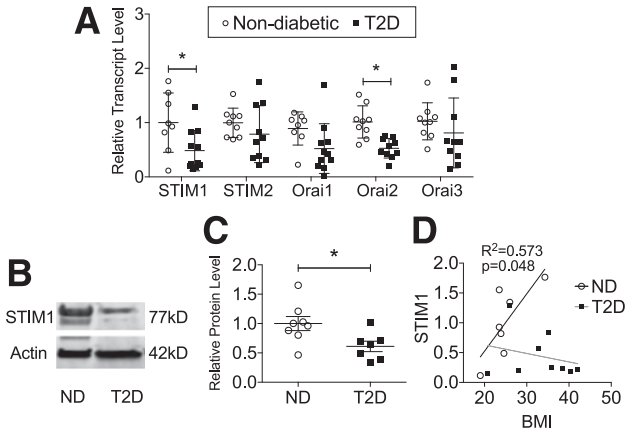

Figure 3—STIM1 expression was reduced in human islets from donors with T2D. Human islets were obtained from seven to nine donors without diabetes (ND donors) and 7–11 donors with T2D. *A*: Total RNA was isolated and subjected to qRT-PCR for quantification of STIM and Orai isoform expression levels. *B* and *C*: Total islet protein was isolated and immunoblot was performed using antibodies against STIM1 and actin. *$P < 0.05$ compared with ND donors. *D*: Correlation analysis between islet STIM1 mRNA levels and donor BMI.

Taken together, our data identified a specific and consistent reduction in STIM1 expression in islets and pancreatic β-cells across a variety of diabetes models. Moreover, pharmacologic inhibition of SOCE reduced GSIS and impaired glucose-stimulated Ca^{2+} oscillations, whereas the effects on calcium oscillations were partially phenocopied by STIM1 knockdown in islets.

STIM1 Deletion Reduced β-Cell SOCE, ER Ca^{2+} Storage, and GSIS

Off-target effects of chemical SOCE inhibitors have been reported (31), including an effect of 2-APB on inositol triphosphate receptor activity. To this end, CRISPR/Cas9 genome editing was used to create an INS-1 STIM1 KO cell line (KO cells). Gene expression analysis of KO cells demonstrated the absence of *STIM1 mRNA*, with no compensatory upregulation of other SOCE constituents including *STIM2* and *Orai1–3* (Fig. 5*A*). In addition, no change in *Serca2b* expression was observed. Similar to the findings observed in our in vitro models of cytokine, GLT, and palmitate-stress, the ΔF response to TG was reduced in STIM1 KO cells (Supplementary Fig. 2*C* and *D*). In addition, SOCE measured in response to TG and carbachol treatment was significantly reduced in KO cells (Fig. 5*B–D*), whereas no further reduction in SOCE was observed when STIM1 KO cells were treated with IL-1β (Supplementary Fig. 3*A* and *B*), GLT (Supplementary Fig. 3*C* and *D*), ML-9, or 2-APB (Supplementary Fig. 3*E*).

To more definitively examine the effect of STIM1 KO on ER Ca^{2+} levels, WT and KO cells were transduced with the ER-targeted, FRET-based, D4ER Cameleon probe, and imaging experiments were performed in Ca^{2+} containing HBSS buffer. Under basal conditions, STIM1KO cells displayed a lower FRET/donor ratio, which is indicative of decreased ER Ca^{2+} levels (Fig. 5*E*). To confirm these findings, FLIM analysis was performed to measure the lifetime of the D4ER cyan fluorescent protein (CFP) donor. As expected, the lifetime of the D4ER donor was increased in KO cells compared with WT cells (Fig. 5*F* and Supplementary Fig. 3*F*). Finally, GSIS was measured in WT and STIM1 KO cells. Similar to results obtained with pharmacologic SOCE inhibition (Fig. 1*D*), STIM1 deletion significantly reduced GSIS, whereas no effect on basal insulin secretion was observed (Fig. 5*G*).

Loss of STIM1 Increased β-Cell ER Stress

We hypothesized reductions in ER Ca^{2+} levels arising from impaired SOCE may likewise impact stress responses in STIM1 KO cells. To test this, WT and KO cells were treated with 25 mmol/L glucose + 0.5 mmol/L palmitate (GLT) or 10 μmol/L TM for 3 h. In response to both GLT and TM, an increase in the spliced/unspliced *XBP-1* ratio was observed in KO cells (Fig. 6*A*). Moreover, STIM1 KO cells exhibited increased cleaved caspase-3 activation in response to IL-1β treatment (Fig. 6*B* and *C*). Next, to compare acute and chronic STIM1 loss, siRNA-mediated STIM1 knockdown was performed in WT INS-1 cells, resulting in an ∼50% reduction in STIM1 gene and protein expression (Fig. 6*D* and *E*). Similar to the results observed in STIM1KO cells, siRNA-treated cells exhibited significantly higher levels of spliced/unspliced *XBP-1* in response to TM treatment (Fig. 6*F*). Finally, to determine whether these functional changes correlated with changes in ER ultrastructure, electron micrographic images of WT and KO cells were analyzed. In contrast to regularly spaced stacks of ER observed in WT cells, the ER was swollen and dilated in STIM1 KO cells (Fig. 6*G*). Taken together, these data indicate that STIM1 loss is associated with changes in ER morphology and increased β-cell susceptibility to TM-, cytokine-, and GLT-mediated stress.

STIM1 Overexpression Restored ER Ca^{2+} Levels and Improved Insulin Secretion in Human Islets From Donors With T2D

To test the effects of STIM1 gain of function, WT and KO cells were transduced with a STIM1-expressing adenovirus, and a dose-dependent increase in STIM1 expression was observed (Fig. 7*A*). Consistent with this, a dose-dependent increase in SOCE was also observed with STIM1 overexpression (Fig. 7*B* and *C*). Next, to test the effect of STIM1 overexpression on ER Ca^{2+} levels, STIM1 KO cells were transduced with the D4ER-expressing adenovirus in combination with either an empty vector or STIM1-expressing adenovirus. Under steady-state conditions, STIM1 restoration led to an increase in the FRET/CFP ratio in KO cells (Fig. 7*D*). This result was confirmed by FLIM analysis, in which the lifetime of the D4ER donor probe was significantly reduced by STIM1 overexpression in KO cells (Fig. 7*E*).

Next, FRET analysis was performed to dynamically monitor ER Ca^{2+} storage in WT and STIM1 KO cells transduced with an empty virus or STIM1-expressing adenovirus. No

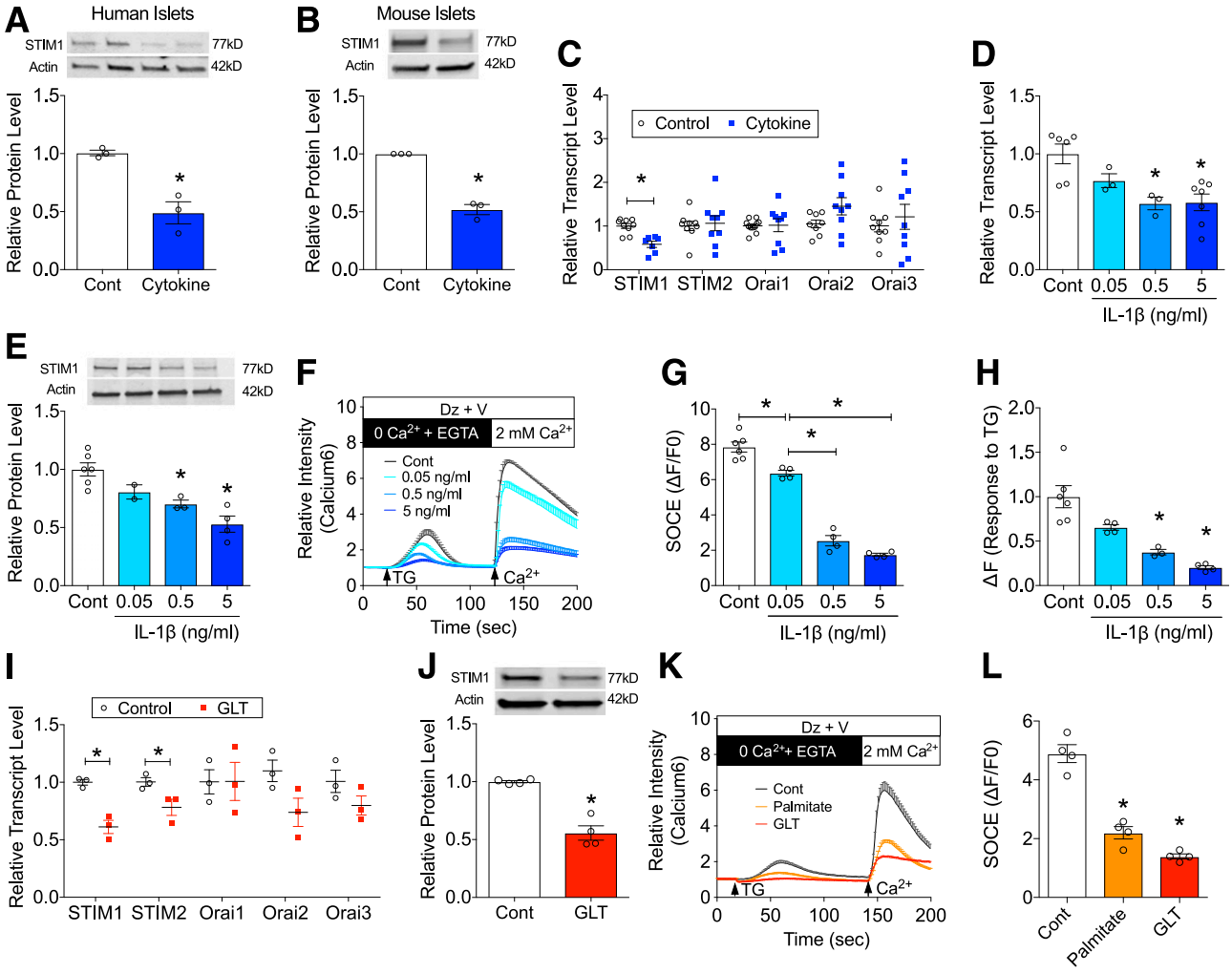

Figure 4—STIM1 expression was decreased under proinflammatory cytokine stress and GLT. Islets from human donors without diabetes (*A*) and C57BL/6J mice (*B*) were treated with 5 ng/mL IL-1β, 100 ng/mL IFN-γ, and 10 ng/mL TNF-α for 24 h. Immunoblot was performed using antibodies against STIM1 and actin. *C*: INS-1 β-cells were treated with 5 ng/mL IL-1β for 24 h; total RNA was isolated and subjected to qRT-PCR for quantification of STIM and Orai isoform mRNA expression levels (normalized to actin mRNA expression). *D–H*: INS-1 β-cells were treated with 0, 0.05, 0.5, or 5 ng/mL IL-1β, for 24 h. Total RNA and protein were isolated and subjected to qRT-PCR for quantification of STIM mRNA (*D*) and protein levels (*E*). *F* and *G*: Cytosolic Ca^{2+} imaging was performed to quantitate SOCE in IL-1β–treated INS-1 cells in the presence of 5.5 mmol/L glucose, 200 μmol/L diazoxide, and 10 μmol/L verapamil (Dz + V). *H*: ER Ca^{2+} levels were indirectly estimated by quantitating the ΔF/F0 response to TG. *I–L*: INS-1 β-cells were treated with a combination of 0.5 mmol/L palmitate + 25 mmol/L glucose (GLT), 0.5 mmol/L palmitate + 11 mmol/L glucose (Palmitate), or vehicle control + 11 mmol/L glucose (Cont) for 24 h (*I*). Total RNA was isolated from control and GLT-treated INS-1 cells and subjected to qRT-PCR for quantification of STIM and Orai mRNA expression levels. *J*: Immunoblot for STIM1 and actin was performed in INS-1 cells treated with GLT for 24 h. *K* and *L*: Cytosolic Ca^{2+} imaging was performed to quantitate SOCE in GLT and palmitate-treated INS-1 cells. The number of replicates for each experiment are indicated by the open circles. *$P < 0.05$ compared with control conditions or for indicated comparisons.

differences in the FRET/CFP ratio were observed at baseline under Ca^{2+}-free conditions. The initial response to carbachol was similar between the groups. In contrast, STIM1 KO cells demonstrated impaired ER Ca^{2+} restoration after ER Ca^{2+} depletion when Ca^{2+} was added to the buffer. Moreover, ER Ca^{2+} restoration was significantly improved in KO cells by STIM1 overexpression (Fig. 7*F–H*).

Next, we tested whether STIM1 overexpression was sufficient to protect against IL-1β–mediated activation of cleaved caspase 3. In both WT and STIM1 KO cells, STIM1 overexpression reduced cleaved caspase 3 protein levels (Fig. 7*I* and *J*). Consistent with this, STIM1 overexpression rescued SOCE under conditions of cytokine stress (Supplementary Fig. 4*A* and *B*). Finally, human cadaveric islets from donors with T2D were transduced with the STIM1-expressing adenovirus or an empty viral control (Fig. 7*K*). Compared with islets transduced with empty virus, GSIS was significantly improved in STIM1-transduced human islets (Fig. 7*L*).

DISCUSSION

Recent findings suggest that ER dysfunction triggers a range of chronic human diseases, including Alzheimer disease, Parkinson disease, atherosclerosis, and diabetes

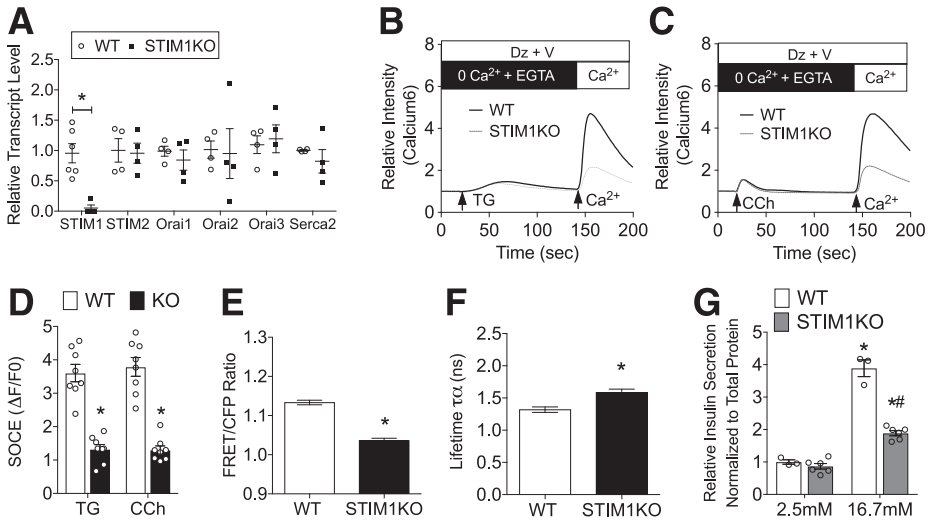

Figure 5—STIM1 deletion led to impaired SOCE, reduced ER Ca^{2+} levels, and decreased GSIS. CRISPR/Cas-9 genomic editing was used to create an INS-1 832/13 STIM1KO cell line. *A*: Total RNA was isolated and subjected to qRT-PCR for quantification of STIM and Orai isoforms and SERCA2b mRNA levels. Numbers of replicates are indicated by the open circles and black squares. Cytosolic Ca^{2+} imaging was performed to quantitate SOCE in STIM1KO and WT cells in response to 3 μmol/L TG (*B*) and 200 μmol/L carbachol (CCh) (*C*), which were used to empty ER Ca^{2+} stores in the presence of 5.5 mmol/L glucose, 200 μmol/L diazoxide, and 10 μmol/L verapamil (Dz + V). *D*: Quantitative assessment of SOCE in WT and KO cells; the numbers of replicates are indicated by the open circles. *E* and *F*: ER Ca^{2+} levels were compared in WT and STIM1KO cells transduced with a D4ER adenovirus, using a confocal microscope imaging system. *E*: FRET/CFP ratios were acquired in HBSS buffer containing 2 mmol/L Ca^{2+} in WT cells (n = 65) and KO cells (n = 53). *F*: Average donor lifetime from FLIM analysis of at least 20 cells from each group. For *A*, *D*, *E*, and *F*, *$P < 0.05$ compared with control WT cells. *G*: GSIS in WT and KO cells was measured and normalized to total protein levels. The number of replicates are indicated by the open circles. *$P <$ 0.05 compared with 2.5 mmol/L glucose; #$P < 0.05$ compared with WT cells treated with 16.7 mmol/L glucose.

(32–35). In the pancreatic β-cell, a key determinant of ER function is the maintenance of robust levels of intraluminal Ca^{2+}, which is required for protein folding and a number of key cellular signaling events. Reductions in β-cell ER Ca^{2+} occur in response to proinflammatory and glucolipotoxic stress and contribute to the pathophysiology of both major forms of diabetes. Under normal conditions, ER Ca^{2+} store depletion triggers a tightly regulated rescue mechanism known as SOCE or Ca^{2+} release-activated Ca^{2+} current. This process was first proposed by Putney (36). However, a complete understanding of the SOCE molecular complex remained elusive until 2005, when STIM1 was identified as the long sought after "ER Ca^{2+} sensor" (8). Since that time, SOCE has been accepted as a predominant pathway of Ca^{2+} entry into nonexcitable cells, where it has been shown to regulate a variety of cellular functions, including proliferation, growth, inflammation, apoptosis, and lipogenesis (14,37). To date, however, a role for SOCE in excitable and secretory cells, including the pancreatic β-cell, has remained incompletely explored.

Here, we show impairment of glucose-stimulated Ca^{2+} oscillations and reduced insulin secretion in response to pharmacologic SOCE inhibition and under conditions of STIM1 loss. Across multiple models of diabetes, our results revealed a preferential reduction in STIM1 mRNA and protein levels in pancreatic islets and β-cells. Furthermore, we show that the genetic loss of STIM1 was sufficient to reduce β-cell SOCE, glucose-stimulated Ca^{2+} oscillations, and insulin secretion, while simultaneously increasing susceptibility to ER stress and cell death in response to glucolipotoxic and proinflammatory conditions. Previously, STIM1, Orai1, and TRPC1 have been identified as key constituents of the β-cell SOCE complex, whereas pharmacologic SOCE inhibition or a dominant-negative form of Orai1 or TRPC1 was shown to reduce insulin secretion in rat islets and clonal β-cell lines (11). Our data highlight an expanded role for STIM1 in nucleating this process and implicate a loss of STIM1 and impaired SOCE in β-cell dysfunction under diabetic conditions.

The impact of altered SOCE on insulin exocytosis is likely to be multifactorial. However, a key finding from our study is that SOCE inhibition and STIM1 loss impaired first-phase glucose-stimulated cytosolic Ca^{2+} responses as well as glucose-induced Ca^{2+} oscillations. These effects were similar to those observed in a mouse model of SERCA2 haploinsufficiency, where reductions in SERCA2 were shown to reduce β-cell ER Ca^{2+} levels and cytosolic Ca^{2+} oscillations (4). Thus, our data offer additional support to the notion that ER Ca^{2+} stores shape the architecture of glucose-induced Ca^{2+} oscillations as well as the β-cell insulin secretory response. Intriguingly, STIM1 was shown recently to interact with the sulfonylurea receptor 1 subunit of the K_{ATP} channel and regulate β-cell K_{ATP} activity in MIN6 cells (19). In this report, short hairpin RNA–mediated STIM1 knockdown reduced K_{ATP} channel activation, whereas STIM1 reconstitution restored K_{ATP} activity, suggesting that reductions in insulin secretion with STIM1 loss/SOCE inhibition may also result from

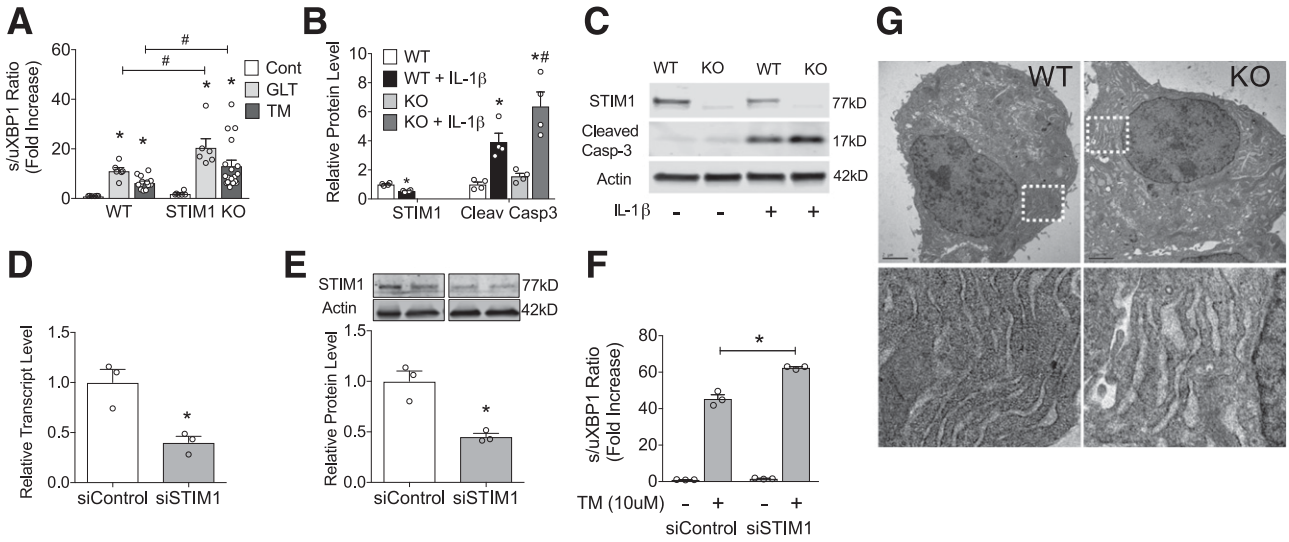

Figure 6—STIM1 deficient cells exhibited increased susceptibility to ER stress. *A*: STIM1KO and WT INS-1 cells were treated with or without 25 mmol/L glucose + 0.5 mmol/L BSA-conjugated palmitate (GLT) or 10 μmol/L TM for 3 h. Total RNA was isolated and subjected to qRT-PCR. Shown are the average spliced/unspliced XBP-1 ratios. *$P < 0.05$, compared with control (Cont) conditions; #$P < 0.05$, for indicated comparisons. *B* and *C*: STIM1KO and WT INS-1 cells were treated with or without 5 ng/mL IL-1β for 24 h. Immunoblot analysis was performed using antibodies against STIM1, cleaved caspase-3, and actin. Quantitative protein levels are shown graphically. *$P < 0.05$ compared with control conditions; #$P < 0.05$ compared with IL-1β–treated WT group. *D* and *E*: INS-1 cells were transfected with siRNAs against STIM1 (siSTIM1) or an siControl. Total RNA and protein were isolated and subjected to qRT-PCR and immunoblot to confirm reduced STIM1 mRNA and protein expression. *F*: siSTIM1- and siControl-transfected cells were treated with 10 μmol/L TM for 3 h, and the spliced/unspliced XBP-1 mRNA ratios were quantitated using qRT-PCR. *$P < 0.05$ compared with control conditions or for indicated comparisons. *G*: STIM1KO and WT INS-1 cells were treated with 10 μmol/L TM for 24 h, fixed, and analyzed by electron microscopy. Representative images of the β-cell ER ultrastructure, indicated by dotted lines in WT and KO cells (scale bars = 2 μm). For each experiment, the numbers of replicates are indicated by the open circles.

impaired K_{ATP} activity (19). A hallmark of advanced human T2D is the development of an impaired response to sulfonylurea medications, which act to close the K_{ATP} channel to increase insulin secretion (38–40). In our data, we observed a positive correlation between donor BMI and STIM1 expression levels in islets from humans without diabetes, but this correlation was lost in donors with T2D. Moreover, our data revealed that STIM1 reconstitution in islets from donors with T2D improved GSIS. These findings imply that STIM1 upregulation may be a compensatory response observed in islets from obese donors that is responsible for the initial maintenance of insulin secretion in the face of advancing insulin resistance. By corollary, our data suggest that reductions in STIM1 could play an important role in the development of impaired insulin secretion and loss of secretagogue efficacy in T2D.

Pathologic reductions in β-cell ER Ca^{2+} levels have been linked with the development of ER stress. Thus, reduced ER Ca^{2+} levels in STIM1-deficient cells led us to hypothesize an additional role for STIM1 in ER stress signaling. Indeed, we found that genetic loss of STIM1 as well as STIM1 knockdown increased β-cell susceptibility to TM-induced ER stress and proinflammatory cytokine–induced cell death. In contrast, STIM1 overexpression was able to protect against proinflammatory cytokine–induced activation of cleaved caspase 3. Recent reports have implicated SERCA2 loss (4,12,41), as well as RyR-mediated ER Ca^{2+} release, in the activation of ER stress signaling in diabetes (13). Here, we have identified an additional role for SOCE dysfunction and STIM1 loss in this phenotype. These observations are in agreement with findings observed in other cell types, including both excitable cells in the central nervous system as well as nonexcitable mouse embryonic fibroblasts (42,43).

Our data revealed a consistent loss of STIM1 in the β-cell across multiple models of diabetes. However, a potential caveat to our observation of reduced STIM1 expression in islets from human donors with T2D is that loss of islet β-cell number may also accompany T2D (44). In addition, STIM1 did not appear as differentially regulated in a microarray analysis of laser-captured islets from human donors with T2D (45). However, we were able to confirm the β-cell downregulation of STIM1 expression using in vitro and ex vivo diabetogenic stress in isolated islets and INS-1 β-cells. Among these models, we found that STIM1 mRNA and protein levels were reduced by proinflammatory cytokines, which are known to be a prominent component of the pathophysiology of type 1 diabetes (46). Additional studies are needed to define whether β-cell SOCE dysregulation may also be present in human type 1 diabetes.

We have not yet explored the intervening pathways that lead to loss of β-cell STIM1 expression under diabetic conditions. In other cell types, the inhibition of both AKT and mammalian target of rapamycin signaling led to a similar loss of STIM1 (47). Notably, both of these

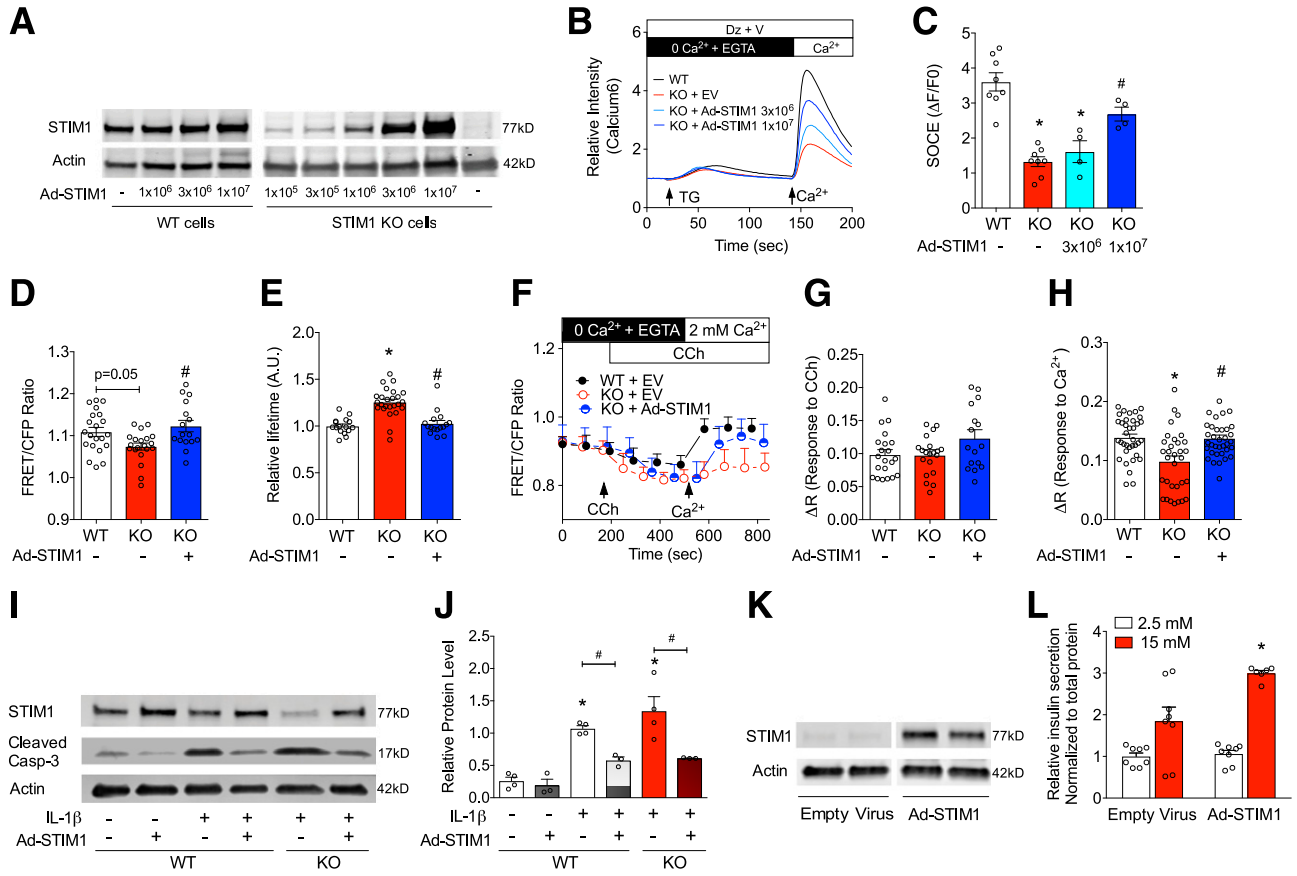

Figure 7—STIM1 overexpression restored ER Ca^{2+} levels and improved insulin secretion in human islets from donors with T2D. *A*: STIM1KO and WT INS-1 cells were transduced with an adenovirus encoding human STIM1 in increasing concentrations (shown as plaque-forming units [pfu]/mL). Immunoblot was performed using antibodies against STIM1 and actin. *B* and *C*: SOCE was measured in STIM1KO cells and WT INS-1 cells that had been transduced with STIM1-expressing adenovirus (Ad-STIM1) or an empty adenoviral control (EV) in the presence of 5.5 mmol/L glucose, 200 μmol/L diazoxide, and 10 μmol/L verapamil (Dz + V). Quantitative results are shown as the ΔF/F0; $*P < 0.05$ compared with WT+EV; $\#P < 0.05$ compared with EV-treated STIM1KO cells. *D–H*: ER Ca^{2+} analysis using FRET and FLIM was performed in D4ER-expressing STIM1KO cells and WT INS-1 cells that had been transduced with Ad-STIM1 or EV. *D*: Quantitation of FRET/CFP ratio of the D4ER probe at baseline in 2 mmol/L Ca^{2+} containing HBSS buffer. *E*: FLIM analysis for the D4ER donor probe is shown graphically as the relative average donor lifetime. For *D* and *E*, $*P < 0.05$ compared with WT cells. $\#P < 0.05$ compared with STIM1 KO cells + EV. *F*: FRET analysis was performed in WT and STIM1 KO cells transduced with Ad-STIM1 or EV in the presence of 5.5 mmol/L glucose. Cch, carbachol. *G* and *H*: Carbachol-induced reductions in ER Ca^{2+} levels and ER Ca^{2+} refilling after the addition of 2 mmol/L Ca^{2+}; results are shown quantitatively as the change in the FRET ratio (ΔR); $*P < 0.05$ compared with WT cells; $\#P < 0.05$ compared with STIM1 KO cells + EV. *I*: STIM1KO cells and WT INS-1 cells were transduced with STIM1-expressing adenovirus or EV control and treated with or without 5 ng/mL IL-1β for 24 h. Immunoblot analysis was performed using antibodies against STIM1, cleaved caspase-3, and actin. *J*: Relative expression levels of cleaved caspase 3 are shown graphically; $*P < 0.05$, compared with control conditions; $\#P < 0.05$ compared for indicated comparisons. *K* and *L*: Human islets from two donors with T2D were transduced with STIM1-expressing adenovirus (3×10^6 pfu/mL) or EV. *K*: Immunoblot was performed to verify STIM1 overexpression. *L*: GSIS from two separate experiments of two donors with four replicates each was measured and normalized to total protein content; $*P < 0.05$ compared with high-glucose conditions in EV-treated islets. For each experiment, the numbers of replicates are indicated by the open circles.

signaling pathways play an essential role in the maintenance of β-cell health and function (48,49). In addition, nuclear factor-κB has been shown to directly bind and modulate STIM1 gene promoter activity in other cell types (50). We and others have previously identified a deleterious effect of nuclear factor-κB–mediated nitric oxide signaling on ER calcium regulation (41,51), and this will be tested in follow-up studies. Here, we focused on the loss of STIM1 expression as the cause of impaired SOCE. However, in other cell types, mislocalization or impaired formation of the SOCE complex has been observed under disease conditions (52). Finally, STIM2 overexpression has been shown to have a strong negative effect on endogenous SOCE in human embryonic kidney 293, PC12, A7r5, and Jurkat T cells (53). Thus, our observation of impaired SOCE in STIM1 KO cells and a reduced Ca^{2+} oscillatory amplitude in STIM1-deleted islets could also be partly explained by alterations in the STIM1/STIM2 ratio.

Notwithstanding these uncertainties, our findings indicate that the loss of STIM1 expression and impaired SOCE in rodent and human models of diabetes resulted in decreased β-cell ER Ca^{2+} levels, increased ER stress, abnormal Ca^{2+} oscillation patterns, and decreased insulin secretion (Fig. 8). The identification of this novel role for

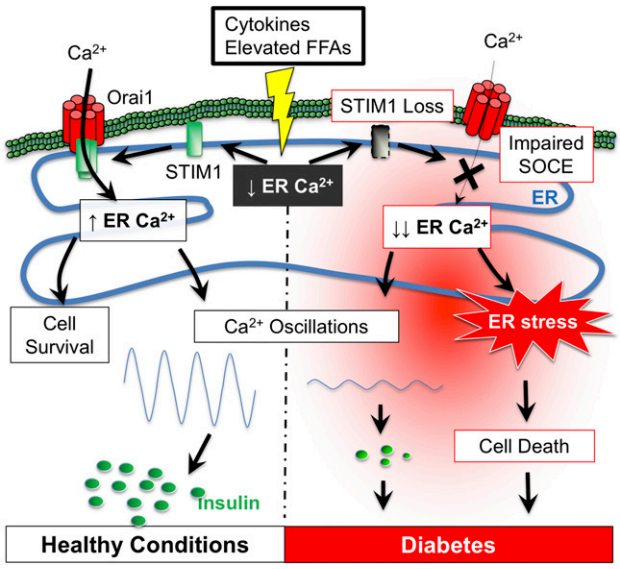

Figure 8—Overall model. Under normal conditions, reductions in ER Ca^{2+} levels are sensed by STIM1, leading to STIM1 oligomerization and translocation to the ER/plasmalemmal junctional regions. Here, STIM1 complexes with selective Orai and TRPC1 channels allow Ca^{2+} influx from the extracellular space, with subsequent transfer of Ca^{2+} into the ER lumen, leading to ER Ca^{2+} restoration. Our study revealed a preferential loss of STIM1 expression under diabetic stress conditions, including exposure to proinflammatory cytokines and elevated free fatty acids. Genetic as well as acquired loss of STIM1 was sufficient to impair β-cell SOCE, reduce ER Ca^{2+} levels, increase β-cell susceptibility to ER stress and death, and cause abnormal glucose-stimulated calcium oscillations and insulin secretory defects. Moreover, our data revealed that STIM1 reconstitution in human cadaveric islets from donors with diabetes was sufficient to improve GSIS, while also protecting against proinflammatory cytokine–induced cell death in INS-1 cells.

STIM1 in the pathogenesis of diabetes suggests that the restoration of STIM1 expression and/or reconstitution of SOCE has the potential to improve β-cell health and function.

Acknowledgments. The authors thank Dr. Richard Day (Indiana University) for helpful advice and technical discussions. The authors also thank Sukrati Kanojia, Preethi Krishnan, Wataru Yamamoto, Morgan Robertson, Gary Considine, Kara Orr, and Daenique Jengelley (Indiana University) for expert technical assistance.

Funding. This work was supported by National Institute of Diabetes and Digestive and Kidney Diseases (NIDDK) grants R01-DK074966 and R01-DK092616 (to M.W.R.), R01-DK-093954 and UC4-DK-104166 (to C.E.-M.), and P30-DK-097512 (Indiana Diabetes Research Center Islet and Physiology, Translation, and Imaging Cores), and gifts from the Sigma Beta Sorority, the Ball Brothers Foundation, the George and Frances Ball Foundation (to C.E.-M.). X.T. was supported by the Diabetes and Obesity DeVault Fellowship at the Indiana University School of Medicine. R.N.B. was supported by National Institutes of Health National Institute Allergy and Infectious Disease Training Grant T32-AI-060519 and a JDRF Postdoctoral Research Award (3-PDF-2017-385-A-N).

The funders had no role in study design, data collection and analysis, decision to publish, or preparation of the manuscript.

Duality of Interest. No potential conflicts of interest relevant to this article were reported.

Author Contributions. T.K. directed the conception and design of the study, the data analysis and interpretation, the collection and assembly of data, and the writing of the manuscript. X.T., S.T., R.N.B., H.I., C.-C.L., and P.S. participated in data collection and critical revision of the manuscript. P.G. and M.W.R. contributed to data analysis, provided critical reagents, and provided critical revision of the manuscript. C.E.-M. directed funding acquisition and study conception and design; participated in the collection and assembly of data; contributed to data analysis; directed the writing of the manuscript; and gave final approval of the manuscript. C.E.-M. is the guarantor of this work and, as such, had full access to all the data in the study and takes responsibility for the integrity of the data and the accuracy of the data analysis.

Prior Presentation. Parts of this study were presented in abstract form at the 76th Scientific Sessions of the American Diabetes Association, New Orleans, LA, 10–14 June 2016, and at the 77th Scientific Sessions of the American Diabetes Association, San Diego, CA, 9–13 June 2017.

References

1. Lytton J, Westlin M, Burk SE, Shull GE, MacLennan DH. Functional comparisons between isoforms of the sarcoplasmic or endoplasmic reticulum family of calcium pumps. J Biol Chem 1992;267:14483–14489
2. Johnson JD, Kuang S, Misler S, Polonsky KS. Ryanodine receptors in human pancreatic beta cells: localization and effects on insulin secretion. FASEB J 2004;18:878–880
3. Gilon P, Chae HY, Rutter GA, Ravier MA. Calcium signaling in pancreatic β-cells in health and in Type 2 diabetes. Cell Calcium 2014;56:340–361
4. Tong X, Kono T, Anderson-Baucum EK, et al. SERCA2 deficiency impairs pancreatic β-cell function in response to diet-induced obesity. Diabetes 2016;65:3039–3052
5. Hogan PG. The STIM1-ORAI1 microdomain. Cell Calcium 2015;58:357–367
6. Takemura H, Putney JW Jr. Capacitative calcium entry in parotid acinar cells. Biochem J 1989;258:409–412
7. Prakriya M, Lewis RS. Store-operated calcium channels. Physiol Rev 2015;95:1383–1436
8. Roos J, DiGregorio PJ, Yeromin AV, et al. STIM1, an essential and conserved component of store-operated Ca2+ channel function. J Cell Biol 2005;169:435–445
9. Prakriya M, Feske S, Gwack Y, Srikanth S, Rao A, Hogan PG. Orai1 is an essential pore subunit of the CRAC channel. Nature 2006;443:230–233
10. Yuan JP, Zeng W, Huang GN, Worley PF, Muallem S. STIM1 heteromultimerizes TRPC channels to determine their function as store-operated channels. Nat Cell Biol 2007;9:636–645
11. Sabourin J, Le Gal L, Saurwein L, Haefliger JA, Raddatz E, Allagnat F. Store-operated Ca2+ entry mediated by orai1 and TRPC1 participates to insulin secretion in rat β-cells. J Biol Chem 2015;290:30530–30539
12. Kono T, Ahn G, Moss DR, et al. PPAR-γ activation restores pancreatic islet SERCA2 levels and prevents β-cell dysfunction under conditions of hyperglycemic and cytokine stress. Mol Endocrinol 2012;26:257–271
13. Santulli G, Pagano G, Sardu C, et al. Calcium release channel RyR2 regulates insulin release and glucose homeostasis [published correction appears in J Clin Invest 2015;125:1968–1978]. J Clin Invest 2015;125:4316
14. Lacruz RS, Feske S. Diseases caused by mutations in ORAI1 and STIM1. Ann N Y Acad Sci 2015;1356:45–79
15. Kraft R. STIM and ORAI proteins in the nervous system. Channels (Austin) 2015;9:245–252
16. Bisaillon JM, Motiani RK, Gonzalez-Cobos JC, et al. Essential role for STIM1/Orai1-mediated calcium influx in PDGF-induced smooth muscle migration. Am J Physiol Cell Physiol 2010;298:C993–C1005
17. Chaudhari S, Ma R. Store-operated calcium entry and diabetic complications. Exp Biol Med (Maywood) 2016;241:343–352
18. Maus M, Cuk M, Patel B, et al. Store-operated Ca^{2+} entry controls induction of lipolysis and the transcriptional reprogramming to lipid metabolism. Cell Metab 2017;25:698–712

19. Leech CA, Kopp RF, Nelson HA, Nandi J, Roe MW. Stromal interaction molecule 1 (STIM1) regulates ATP-sensitive potassium (K_{ATP}) and store-operated Ca^{2+} channels in MIN6 β-cells. J Biol Chem 2017;292:2266–2277
20. Ogihara T, Chuang JC, Vestermark GL, et al. Liver X receptor agonists augment human islet function through activation of anaplerotic pathways and glycerolipid/free fatty acid cycling. J Biol Chem 2010;285:5392–5404
21. Evans-Molina C, Robbins RD, Kono T, et al. Peroxisome proliferator-activated receptor gamma activation restores islet function in diabetic mice through reduction of endoplasmic reticulum stress and maintenance of euchromatin structure. Mol Cell Biol 2009;29:2053–2067
22. Imai Y, Fink BD, Promes JA, Kulkarni CA, Kerns RJ, Sivitz WI. Effect of a mitochondrial-targeted coenzyme Q analog on pancreatic β-cell function and energetics in high fat fed obese mice. Pharmacol Res Perspect 2018;6:e00393
23. Johnson JS, Kono T, Tong X, et al. Pancreatic and duodenal homeobox protein 1 (Pdx-1) maintains endoplasmic reticulum calcium levels through transcriptional regulation of sarco-endoplasmic reticulum calcium ATPase 2b (SERCA2b) in the islet β cell. J Biol Chem 2014;289:32798–32810
24. Carter JD, Dula SB, Corbin KL, Wu R, Nunemaker CS. A practical guide to rodent islet isolation and assessment. Biol Proced Online 2009;11:3–31
25. Hum JM, Siegel AP, Pavalko FM, Day RN. Monitoring biosensor activity in living cells with fluorescence lifetime imaging microscopy. Int J Mol Sci 2012;13:14385–14400
26. Dyachok O, Gylfe E. Store-operated influx of Ca(2+) in pancreatic beta-cells exhibits graded dependence on the filling of the endoplasmic reticulum. J Cell Sci 2001;114:2179–2186
27. Smyth JT, Dehaven WI, Bird GS, Putney JW Jr. Ca2+-store-dependent and -independent reversal of Stim1 localization and function. J Cell Sci 2008;121:762–772
28. Oh-Hora M, Yamashita M, Hogan PG, et al. Dual functions for the endoplasmic reticulum calcium sensors STIM1 and STIM2 in T cell activation and tolerance. Nat Immunol 2008;9:432–443
29. Varga-Szabo D, Braun A, Kleinschnitz C, et al. The calcium sensor STIM1 is an essential mediator of arterial thrombosis and ischemic brain infarction. J Exp Med 2008;205:1583–1591
30. Miani M, Colli ML, Ladrière L, Cnop M, Eizirik DL. Mild endoplasmic reticulum stress augments the proinflammatory effect of IL-1β in pancreatic rat β-cells via the IRE1α/XBP1s pathway. Endocrinology 2012;153:3017–3028
31. Saleem H, Tovey SC, Molinski TF, Taylor CW. Interactions of antagonists with subtypes of inositol 1,4,5-trisphosphate (IP3) receptor. Br J Pharmacol 2014;171:3298–3312
32. Hetz C, Chevet E, Harding HP. Targeting the unfolded protein response in disease. Nat Rev Drug Discov 2013;12:703–719
33. Sammels E, Parys JB, Missiaen L, De Smedt H, Bultynck G. Intracellular Ca2+ storage in health and disease: a dynamic equilibrium. Cell Calcium 2010;47:297–314
34. Ozcan L, Tabas I. Role of endoplasmic reticulum stress in metabolic disease and other disorders. Annu Rev Med 2012;63:317–328
35. Wang S, Kaufman RJ. The impact of the unfolded protein response on human disease. J Cell Biol 2012;197:857–867
36. Putney JW Jr. A model for receptor-regulated calcium entry. Cell Calcium 1986;7:1–12
37. Soboloff J, Rothberg BS, Madesh M, Gill DL. STIM proteins: dynamic calcium signal transducers. Nat Rev Mol Cell Biol 2012;13:549–565
38. Turner RC, Holman RR. Lessons from UK prospective diabetes study. Diabetes Res Clin Pract 1995;28(Suppl.):S151–S157
39. Turner RC, Cull CA, Frighi V, Holman RR. Glycemic control with diet, sulfonylurea, metformin, or insulin in patients with type 2 diabetes mellitus: progressive requirement for multiple therapies (UKPDS 49). UK Prospective Diabetes Study (UKPDS) Group. JAMA 1999;281:2005–2012
40. Del Prato S, Nauck M, Durán-Garcia S, et al. Long-term glycaemic response and tolerability of dapagliflozin versus a sulphonylurea as add-on therapy to metformin in patients with type 2 diabetes: 4-year data. Diabetes Obes Metab 2015;17:581–590
41. Cardozo AK, Ortis F, Storling J, et al. Cytokines downregulate the sarcoendoplasmic reticulum pump Ca2+ ATPase 2b and deplete endoplasmic reticulum Ca2+, leading to induction of endoplasmic reticulum stress in pancreatic beta-cells. Diabetes 2005;54:452–461
42. Selvaraj S, Sun Y, Watt JA, et al. Neurotoxin-induced ER stress in mouse dopaminergic neurons involves downregulation of TRPC1 and inhibition of AKT/mTOR signaling. J Clin Invest 2012;122:1354–1367
43. Henke N, Albrecht P, Pfeiffer A, Toutzaris D, Zanger K, Methner A. Stromal interaction molecule 1 (STIM1) is involved in the regulation of mitochondrial shape and bioenergetics and plays a role in oxidative stress. J Biol Chem 2012;287:42042–42052
44. Kilimnik G, Zhao B, Jo J, et al. Altered islet composition and disproportionate loss of large islets in patients with type 2 diabetes. PLoS One 2011;6:e27445
45. Marselli L, Thorne J, Dahiya S, et al. Gene expression profiles of Beta-cell enriched tissue obtained by laser capture microdissection from subjects with type 2 diabetes. PLoS One 2010;5:e11499
46. Eizirik DL, Colli ML, Ortis F. The role of inflammation in insulitis and beta-cell loss in type 1 diabetes. Nat Rev Endocrinol 2009;5:219–226
47. Ogawa A, Firth AL, Smith KA, Maliakal MV, Yuan JX. PDGF enhances store-operated Ca2+ entry by upregulating STIM1/Orai1 via activation of Akt/mTOR in human pulmonary arterial smooth muscle cells. Am J Physiol Cell Physiol 2012;302:C405–C411
48. Prentki M, Nolan CJ. Islet beta cell failure in type 2 diabetes. J Clin Invest 2006;116:1802–1812
49. Elghazi L, Rachdi L, Weiss AJ, Cras-Méneur C, Bernal-Mizrachi E. Regulation of beta-cell mass and function by the Akt/protein kinase B signalling pathway. Diabetes Obes Metab 2007;9(Suppl. 2):147–157
50. DebRoy A, Vogel SM, Soni D, Sundivakkam PC, Malik AB, Tiruppathi C. Cooperative signaling via transcription factors NF-κB and AP1/c-Fos mediates endothelial cell STIM1 expression and hyperpermeability in response to endotoxin. J Biol Chem 2014;289:24188–24201
51. Tong X, Kono T, Evans-Molina C. Nitric oxide stress and activation of AMP-activated protein kinase impair β-cell sarcoendoplasmic reticulum calcium ATPase 2b activity and protein stability. Cell Death Dis 2015;6:e1790
52. Xu S, Nam SM, Kim JH, et al. Palmitate induces ER calcium depletion and apoptosis in mouse podocytes subsequent to mitochondrial oxidative stress. Cell Death Dis 2015;6:e1976
53. Soboloff J, Spassova MA, Hewavitharana T, et al. STIM2 is an inhibitor of STIM1-mediated store-operated Ca2+ entry. Curr Biol 2006;16:1465–1470